Publishing House
AKAPIT

COMPUTER METHODS IN MATERIALS SCIENCE

Informatyka w Technologii Materiałów

Vol. 14, 2014, No. 1

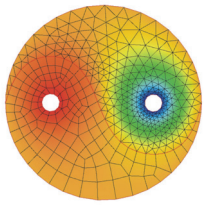

EXPERIMENTAL VERIFICATION AND VALIDATION OF THE PHASE TRANSFORMATION MODEL USED FOR OPTIMIZATION OF HEAT TREATMENT OF RAILS

ROMAN KUZIAK[1]*, RYSZARD MOLENDA[1], ANDRZEJ WROŻYNA[1], JAN KUSIAK[2], MACIEJ PIETRZYK[2]

[1]Institute for Ferrous Metallurgy, ul. K. Miarki 12, 44-100 Gliwice, Poland
[2]AGH University of Science and Technology, al. Mickiewicza 30, 30-059 Kraków, Poland
**Corresponding author: rkuziak@imz.pl*

Abstract

Dilatometric tests for the eutectoid steel were performed and the results were used for identification of the phase transformation model for this steel. Physical simulations of controlled heat treatment of rail head were performed. Microstructure and properties after various thermal cycles were determined and these data were used to validate the model of controlled cooling of rails. As a consequence, a reliable model which predicts temperature field during cooling, kinetics of phase transformations, microstructural parameters and mechanical properties of the product was developed. This model can be applied to solve the optimization task formulated with the objective of searching for the cooling process parameters, which give as low as possible interlamellar spacing in pearlite, microstructure free of bainite and heterogeneous hardness distribution in the rail head.

Key words: pearlitic steels, rails, controlled cooling, modelling, validation

1. INTRODUCTION

The constant development of rail transport is specifically connected with an increase in train speed, application of greater axle loads due to an increase in the weight of materials carried by rail transport, as well as linking of the railway networks with the tram infrastructure. Over the last decades a constant progress has been made in the rail transportation sector. The rail transport capacities depend strongly on such track parameters as car stability, geometry of the contact with running wheel, and possibility to sustain greater loads (Kuziak & Zygmunt, 2012). Quality of rails is characterized by the increased wear resistance, fatigue strength and resistance to contact-fatigue defects occurrence. This features can be obtained for pearlite structure after accelerated cooling giving small distance between the cementite lamellae (S_0 around 0.10-0.12 μm), as compared to the structure after the natural cooling in the air (S_0 around 0.2-0.3 μm) (Kuziak & Zygmunt, 2012). Reduction of the distance between lamellae results in an increase of pearlite strength/hardness (Kuziak et al., 1997; Kuziak & Zygmunt, 2012). Simultaneously, it results in thinning of cementite lamellae, which increases plasticity of this phase.

Problem of heat treatment of rails directly after hot rolling has been in the field of interest of scientist for some time. Numerous papers dealing with the phenomena of heat transfer (Ackert & Nott, 1987; Morales et al., 1990; Sahay et al., 2009) microstructure evolution (Perez-Unzueta & Beynon, 1993) and thermal stresses (Boyadiev et al., 1996) can be found in the scientific literature. Intensive researches aimed at designing of new method of pearlitic rails head hardening process giving rise to substantial

 ISSN 1641-8581

progress in reducing of the interlamellar spacing of cementite lamellae and the size of pearlite colony as compared to the these parameters after cooling in still air have been conducted by Kuziak & Zygmunt (2012). Beyond this, various researchers have developed models describing kinetics of phase transformation for eutectoid steels to be adopted into the continuous cooling conditions using additivity rule. These models allow description of such features of the austenite decomposition in eutectoid steels as the transformations start and end temperature, as well as volume fractions of structural components. More advanced models can predict such specific features of the pearlitic microstructure as grain size, colony size and interlamellar spacing, see for example Authors paper (Pietrzyk & Kuziak, 2000). This model was applied by Pietrzyk and Kuziak (2012) to simulation of controlled cooling of rail head. Accuracy of the models is limited due to number of parameters, which are difficult to determine. Therefore, the objective of this paper was physical simulation of the controlled cooling of rails and supplying data for the verification and validation of the model.

2. MICROSTRUCTURE EVOLUTION AND MECHANICAL PROPERTIES MODELS FOR EUTECTOID STEELS

The models, which will be used in optimization of the controlled cooling of rails, are divided into finite element model of temperature changes, phase transformations model, microstructure model and mechanical properties model. The FE heat transfer model is Authors FE code described by Lenard et al. (1999) and it is not presented in this paper. The remaining three models are also described in previous publications, but they repeated briefly below.

2.1. Phase transformation model

Detailed description of this model can be found in (Pietrzyk & Kuziak, 2000; 2012). Briefly, the kinetics of the pearlitic and bainitic transformations is described by the JMAK (Johnson, Mehl, Avrami, Kolmogorov) type equation:

$$X = 1 - \exp\left(-kt^n\right) \tag{1}$$

where: X – transformed volume fraction, k, n – coefficients, t – time.

Scheil (1935) additivity rule was applied to account for the temperature changes during transformations. Incubation time for pearlitic and bainitic transformation is acounted for:

$$\text{pearlite: } \tau_P = \frac{a_1}{\left(\mathrm{Ae}_1 - T\right)^{a_3}} \exp\left[\frac{a_2 \times 10^3}{R\left(T+273\right)}\right] \tag{2}$$

$$\text{bainite: } \tau_b = \frac{a_9}{\left(a_{12} - T\right)^{a_{11}}} \exp\left[\frac{a_{10} \times 10^3}{R\left(T+273\right)}\right] \tag{3}$$

where: T – temperature in ^{o}C, R – gas constant.

Constant value of coefficient n in equation (1) is used. The values of n are introduced in the model as a_4 and a_{13} for pearlitic and bainitic transformations, respectively. Coefficient k is defined as a temperature function:

$$\text{pearlite: } \quad k = \frac{a_7}{D_\gamma^{a_8}} \exp\left(a_6 - \frac{a_5 T}{100}\right) \tag{4}$$

$$\text{bainite: } \quad k = a_{17} \exp\left(a_{16} - \frac{a_{15} T}{100}\right) \tag{5}$$

where: D – grain size.

Remaining equations in the model are:

– Start temperature for bainitic transformation:

$$B_s = a_{13} - 425[\mathrm{C}] - 42.5[\mathrm{Mn}] - 31.5[\mathrm{Ni}] \tag{6}$$

– Start temperature for martensitic transformation:

$$M_s = a_{18} - a_{19} c_\gamma \tag{7}$$

Volume fraction of the martensite is calculated according to the model of Koistinen and Marburger (1959), described also in (Umemoto et al., 1992; Pietrzyk et al., 2003):

$$F_m = \left(1 - F_p - F_b\right)\left\{1 - \exp\left[-0.011\left(M_s - T\right)\right]\right\} \tag{8}$$

where: F_p, F_b – volume fractions of pearlite and bainite with respect to the whole volume of the sample, M_s – martensite start temperature.

This model was applied to simulations of controlled cooling of rails.

2.2. Model of microstructure and properties

Details of this model are given in publications (Kuziak et al., 1997; Pietrzyk & Kuziak, 2000; 2012). The model includes equations, which describe microstructural parameters of eutectoid steel after cooling from austenite stability temperature to the room temperature. The resulting microstructure is composed of pearlite nodes subdivided into colo-

nies in the process of pearlite growth. Typically, there are several colonies in pearlite nodules, characterized by parallel orientation of the cementite/ferrite lamellae within each colony. Pearlite microstructure composed of nodules subdivided into colonies is formed when austenite grains before the transformation are relatively large (≥ 20 μm), and pearlitic transformation occurs with minor undercooling with respect to the temperature Ae_1. For smaller austenite grains and considerable undercooling of austenite at the beginning of transformation, the difference between the nodules and pearlite colonies disappears and such microstructure was called a colonial pearlite by Garbarz & Pickering (1988).

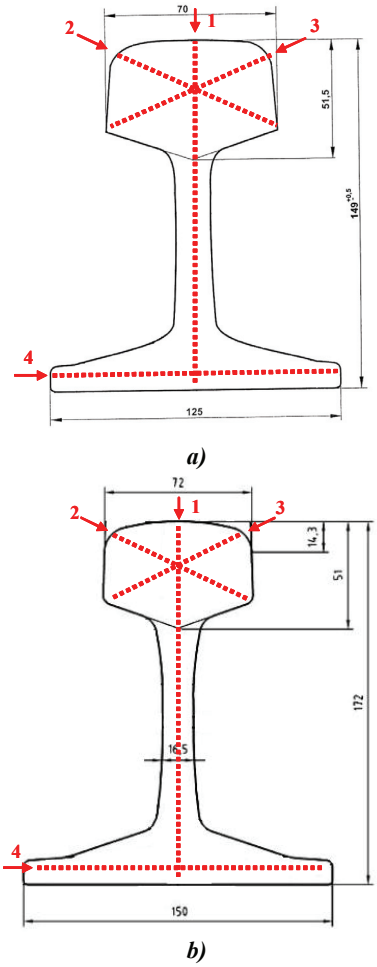

Fig. 1. Cross sections of the rails S49 (a) and UIC60 (b) with the locations of the hardness measurements.

The spacing between cementite lamellae is the most important parameter characterizing pearlite microstructure. The running surface of rail head is of particular interest. Fine pearlite should be a dominant component of this layer. The interlamellar spacing in pearlite, in μm, is calculated as:

$$S_0 = \frac{1}{a - bT_p}$$
$$a = 129.3 - 54.4[\mathrm{Mn}] - 4.38[\mathrm{Cr}] - 17.5[\mathrm{Si}]$$
$$b = 0.178 - 0.072[\mathrm{Mn}] - 0.012[\mathrm{Cr}] - 0.0274[\mathrm{Si}] \quad (9)$$

where: T_p – temperature of pearlitic transformation in ºC, [Mn], [Cr], [Si], [C] – manganese, chromium, silicon and carbon content in wt%.

Since the temperature varies during cooling, the interlamellar spacing is calculated for weighted average temperature during the transformation. Pearlite grain size (D_p) and pearlite colony size (D_c) are two additional parameters included in the model. They are calculated from the following equations (Pietrzyk & Kuziak, 2000; 2012):

$$D_p = \frac{6500\left[1 - \exp\left(-0.016 D_\gamma\right)\right]^{0.6}}{\mathrm{Ae}_1 - T_p} \quad (10)$$

$$D_c = \frac{1}{0.857 - 0.00119 T_p} \quad (11)$$

where: T_p – average temperature of pearlitic transformation in ºC.

Equations, which describe mechanical properties of eutectoid steel in the room temperature, are included in the model, as well. Yield stress ($R_{0.2}$) and tensile strength (R_m) in MPa for eutectoid steel are calculated as (Pietrzyk & Kuziak, 2012; Kuziak & Zygmunt, 2013):

$$R_{0.2} = 259 + 0.087\chi^{-1}$$
$$R_m = 793 + 0.07\chi^{-1} + 122[\mathrm{Si}] \quad (12)$$

where: $\chi = (2S_0 - t)$ - the mean free path for dislocation glide in pearlitic ferrite, t - thickness of the cementite plate calculated as $0.015S_0$[C], [Si], [C] – silicon and carbon content in wght%.

The wear resistance of pearlitic rails is directly linked with their hardness. Increasing the hardness causes the wear resistance increase. The Brinell hardness can approximately be calculated as HB = $0.27R_m$ (Kuziak & Zygmunt, 2013).

3. PHYSICAL SIMULATION OF THE CONTROLLED COOLING OF RAILS AND VALIDATION OF MODELS

The chemical composition of experimental steel grade 900A was as follows: 0.71%C, 1.1%Mn, 0.31%Si, and 0.13%Cr. 500 mm long pieces of the

rails S49 and UIC60 were tested. Cross sections of these rails with the locations of the hardness measurements is shown in figure 1.

3.1. Identification of the phase transformation model

Dilatometric tests were performed for the investigated steel and the inverse analysis was applied to identify coefficients $\mathbf{a} = \{a_1, \ldots, a_{19}\}$ in the model. Inverse algorithm proposed in (Szeliga et al., 2006) and applied by Pietrzyk et al. (2000) to dilatometric tests was used by Pietrzyk & Kuziak (2012) for the investigated steel 900A. Coefficients **a** determined for this steel are given in (Pietrzyk & Kuziak, 2012). Performed in that work comparison between measured and calculated start and end temperatures for phase transformations confirmed good predictive capability of the model.

ThermoCalc software was used to determine equilibrium carbon concentrations. The following relations were obtained for the investigated steel:

$$\begin{aligned} c_{\gamma\beta} &= -1.46583 + 0.002887T \\ c_{\gamma\alpha} &= 4.8513 - 0.005776T \end{aligned} \tag{13}$$

where: $c_{\gamma\alpha}$ - carbon content at the γ/α interface, $c_{\gamma\beta}$ - carbon content at the γ/*cementite* interface, T - temperature in ^{o}C.

The system for water spray cooling contains 4 sections of nozzles with 1 to 8 nozzles in each section. Positions and angles of nozzles can be controlled. Distance between the nozzle and the surface of the rail can be changed in the range of 5 to 200 mm. All cooling parameters are automatically computer controlled. Beyond this, the velocity of the rails movement through the nozzles can be changed in the range of 0.1 - 1m/s. In consequence, wide possibilities of control of the intensity of cooling exist in the system.

The motion of the rail is controlled by the computer and the whole cooling process is monitored with the sampling frequency 100 Hz. Temperature is measured by the thermocouples at 8 locations in the rail. Schematic illustration of the water spray cooling system is shown in figure 2.

The system for cooling by immersion in the polymer solution allows subsequent accelerated (immersion) and slow (in the air) cooling stages. The cooling sequence can be programmed in the computer. View of the system of cooling by immersion in the polymer solution is shown in figure 3.

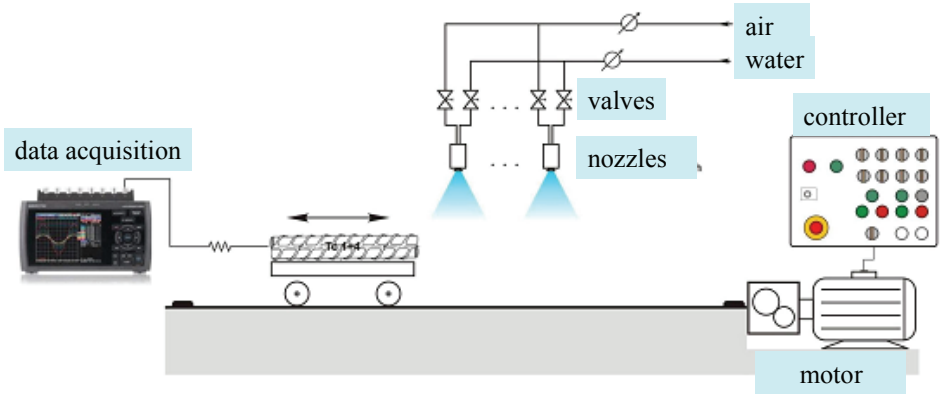

Fig. 2. *Schematic illustration of the system for cooling of the rail head with the water spray.*

3.2. Controlled cooling experimental setup

Semi-industrial heat treatment device, which was built at IMŻ Gliwice, allows the following methods of cooling:

- water spray,
- water-air mist,
- air under pressure,
- immersion in the water-polymer solution.

3.3. Results of physical simulations and verification and validation of models

Both methods of cooling, water spray and immersion in the polymer solution, were used in the physical simulations. However, for the sake of the thermal-microstructural model capability illustration, the latter cooling method only are presented in this paper. 15% water solution of the polymer was

used as coolant. The rails were preheated at 950ºC for 30 min. After cooling mechanical properties were determined according to the standard EN 13674-1 and distribution of the hardness was measured along the lines in figure 1. Beyond this, the microstructure at the cross section was analyzed using optical and scanning microscopes.

a)

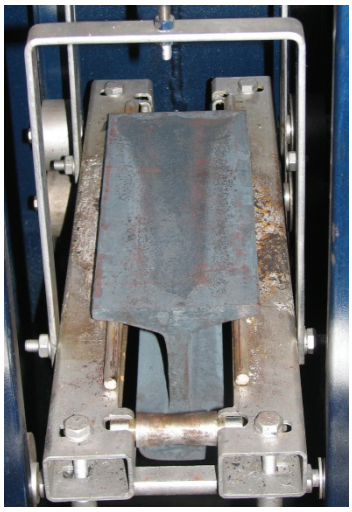

b)

Fig. 3. *General view of the system for cooling of the rail head by immersion in the polymer solution (a) and method of the assembly of the rail in this system (b).*

Several thermal cycles were investigated and four of them are discussed in this paper. Changes of the position of the rail head as a function of time during various cooling cycles are shown in figure 4. Tests 1 and 2 were performed for the rail S49. In the test 2, the last immersion was longer comparing to the test 1. Similarly tests 3 and 4 were applied to the rail UCI60. Measured temperatures during these cycles were compared with the results of calculation and selected results of this comparison for the rail S49 are show in figure 5. Three thermocouples were located at the distance 2 mm (A), 6 mm (B) and 16 mm (C) below the surface of the head. Thermocouples were inserted in the orifices drilled through the rail from the foot. According to Pietrzyk & Kuziak (2012), the heat transfer coefficient for the steel immersed in the polymer solution was 1700 W/m^{2}K at surface temperatures exceeding 700^{o}C. When temperature was decreasing below 700^{o}C, the heat transfer coefficient was increasing and reached the maximum value of 2400 W/m^{2}K at 300^{o}C. Further decrease of the temperature resulted in the decrease of the heat transfer coefficient to the value of 1200 W/m^{2}K at ambient temperature. Analysis of these results shows that the general trend of temperature changes is predicted very well, however, the model predicts sharper changes of the slope of the time-temperature curve at the location close to the surface (A), comparing to measurements. It may be due to smoothing of the temperature changes by the measuring system, as well as to oxidation of the steel surface. Similar results were obtained for the remaining tests. In general it can be concluded that accuracy of the model and assumption of the heat transfer coefficient was confirmed.

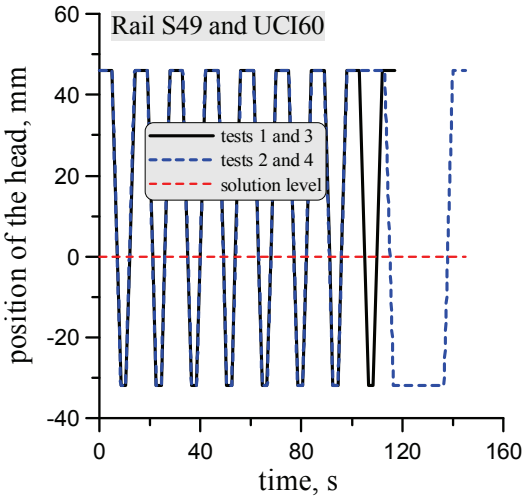

Fig. 4. *Position of the head as a function of time during various cooling schedules for the rail S49 (a) and UCI60 (b).*

Mechanical properties of rails after cooling were measured according to the standard EN 13674-1. Locations where samples were taken are shown in figure 6. Results of mechanical tests are presented in figure 7. Results for the rail cooled by water spray are marked with „D".Measured yield stress and ultimate tensile strength were compared with the results of calculations and good agreement was obtained for all cooling variants.

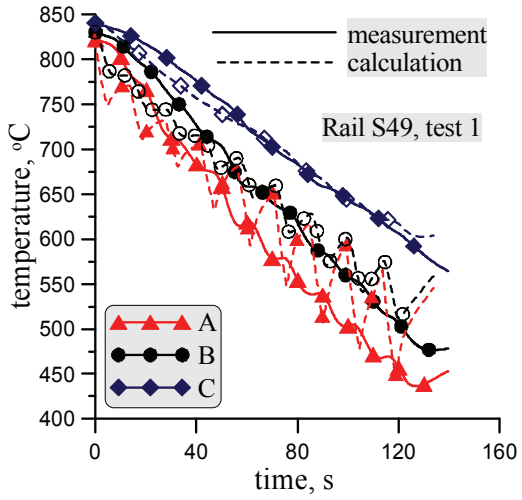

a)

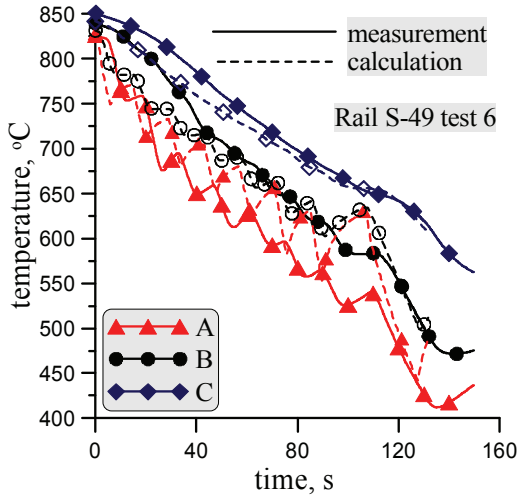

b)

Fig. 5. *Selected results of comparison of measured (full symbols and solid line) and calculated (open symbols and dotted line) temperatures for the rail S49. Temperature after the last immersion 436°C (a) and 412°C (b).*

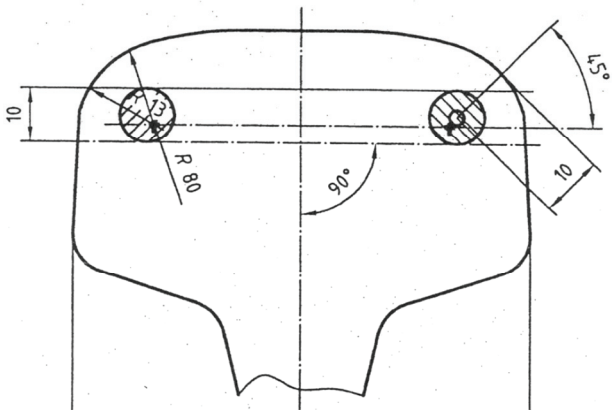

Fig. 6. *Locations at the rail cross section where the samples for mechanical tests were taken.*

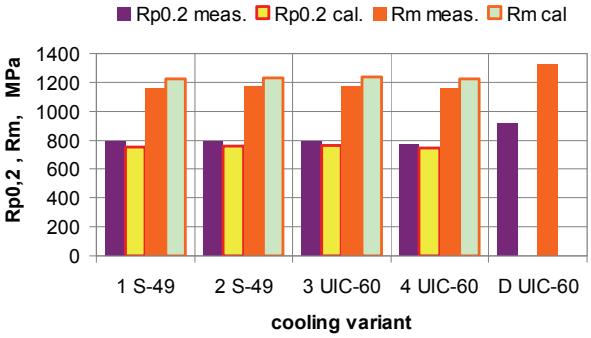

a)

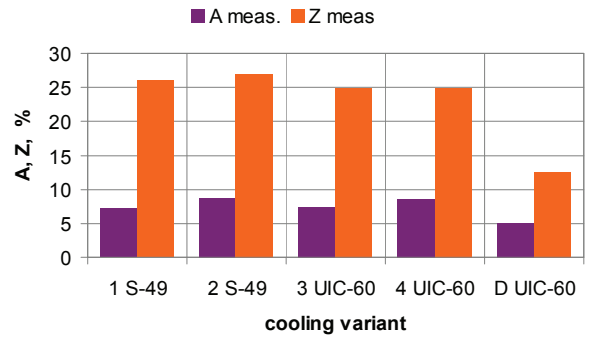

b)

Fig. 7. *Selected results of the mechanical tests, yield stress and ultimate tensile strength A (a) and elongation and reduction in the area Z (b).*

To avoid the influence of the decarburizing at the head surface, the microstructure was analyzed for the samples, which were cut for the mechanical tests at locations in figure 6. Figures 7-9 show microstructures of rails cooled using the immersion in the polymer solution. Micrographs were taken at the distance *d* from the surface specified in the description of figures 8 and 10. Beyond the samples taken close to the surface, all remaining microstructures contain fine pearlite. The best microstructures were obtained for test 6 for the rail S49 and for the test 2 for the rail UIC60. Due to the decarburizing, some ferrite located at the boundaries of previous austenite grains was observed in the areas close to the head surface. Some bainite grains can be found in this microstructure, as well.

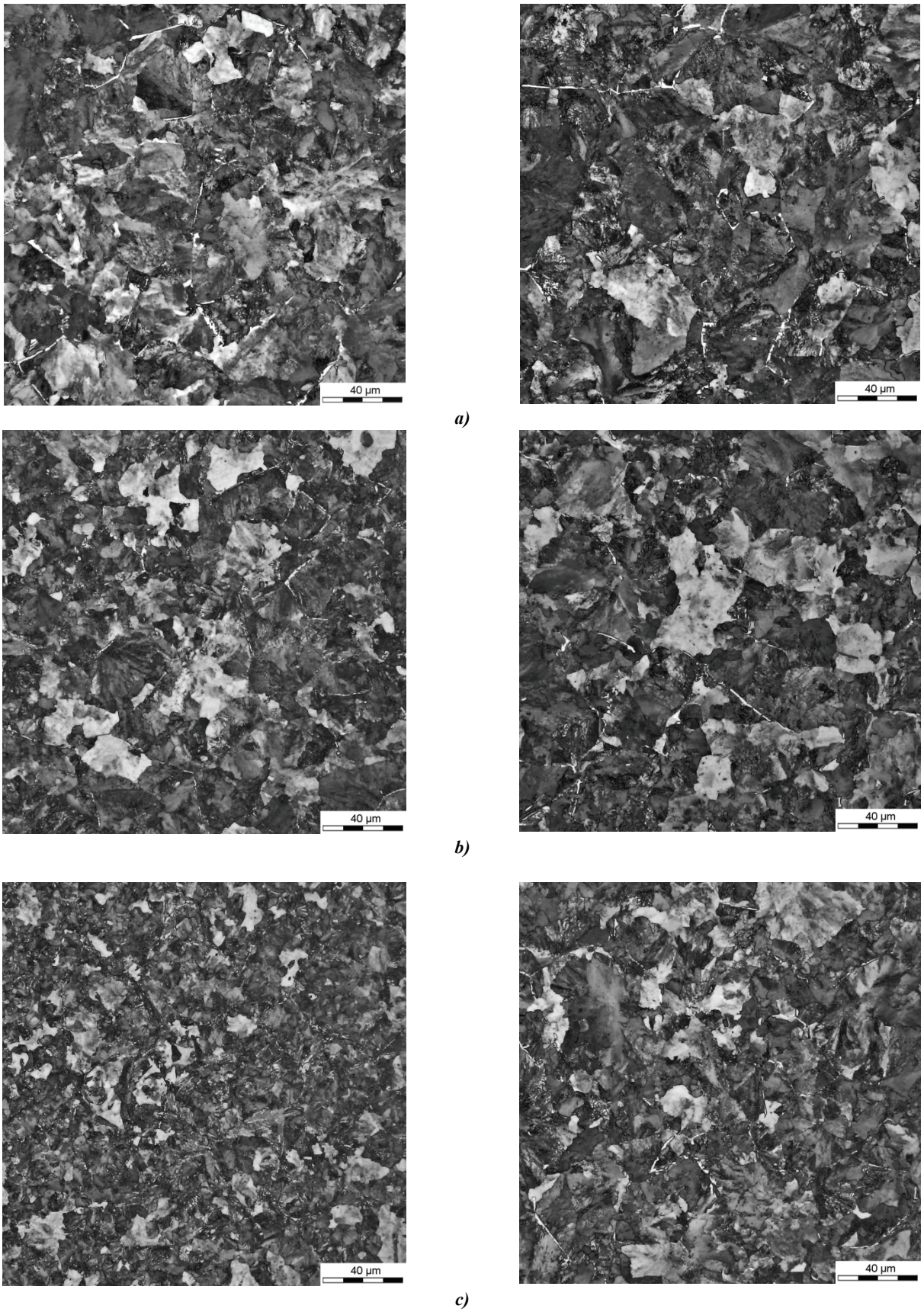

Fig. 8. *Microstructures for the rail S-49 at the distance d = a) 18 mm; b) 6 mm; c) 2mm; for the tests 1 (left) and 2 (right) – optical microscopy.*

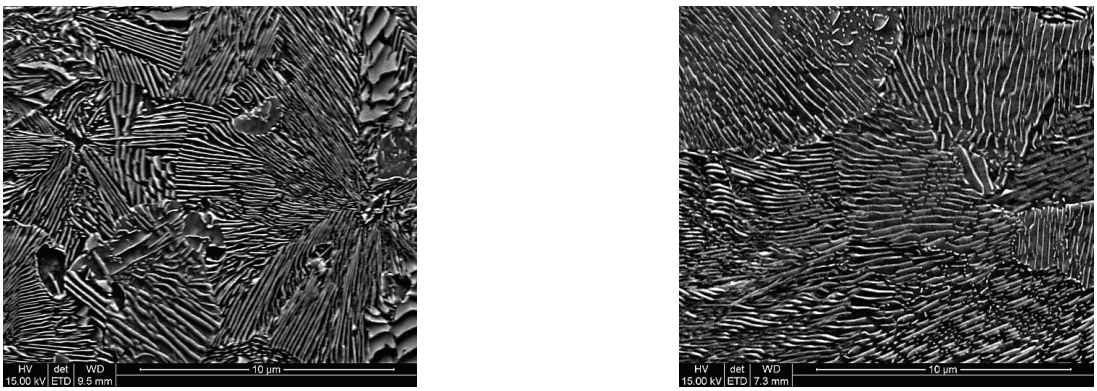

a) *b)*

Fig. 9. *Microstructures for the rail S-49 for the tests 1 (a) and 2 (b) – scanning microscopy.*

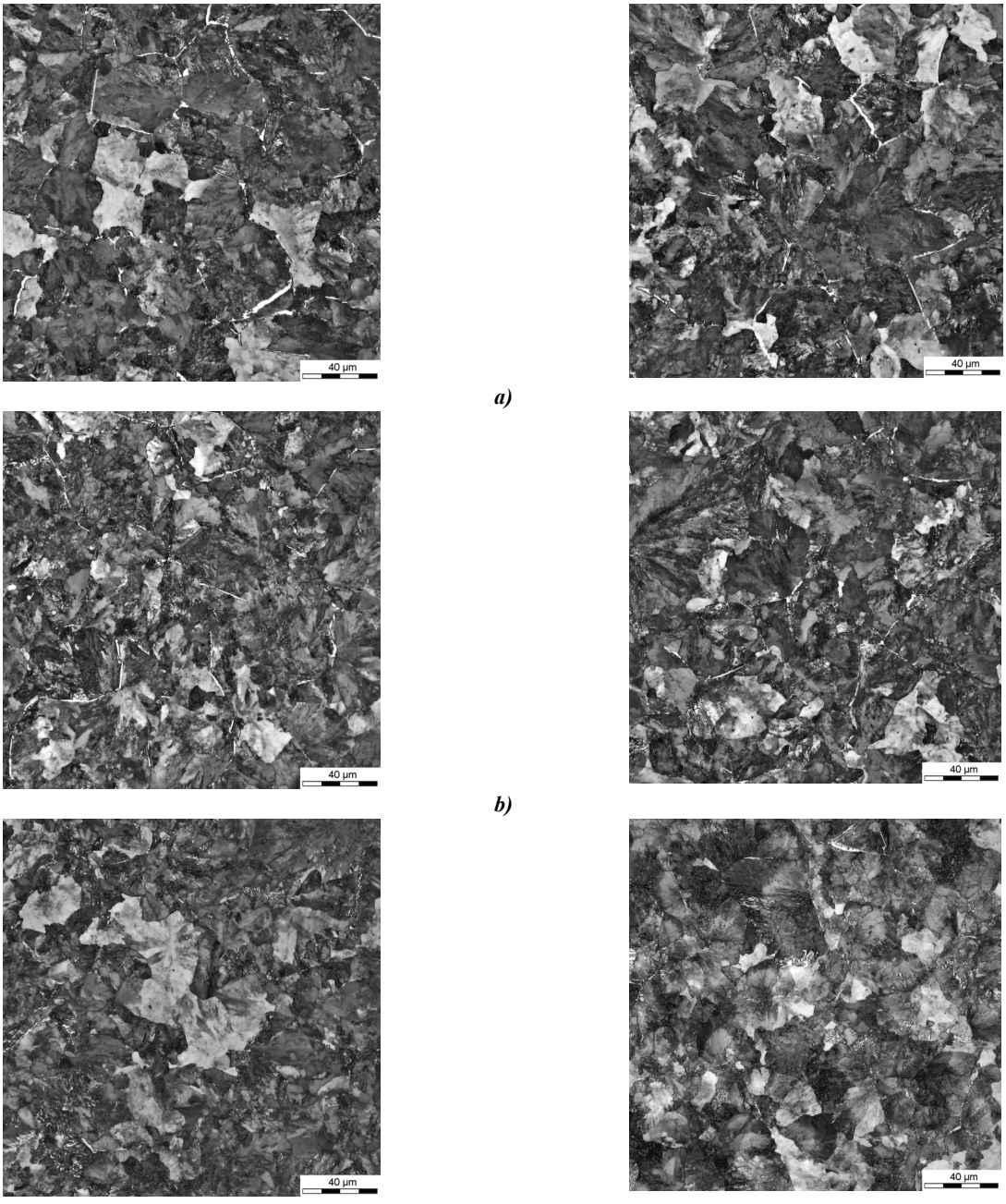

a)

b)

c)

Fig. 10. *Microstructures for the rail UIC60 at the distance d = a) 18 mm; b) 6 mm; c) 2mm; for the tests 3 (left) and 4 (right) – optical microscopy.*

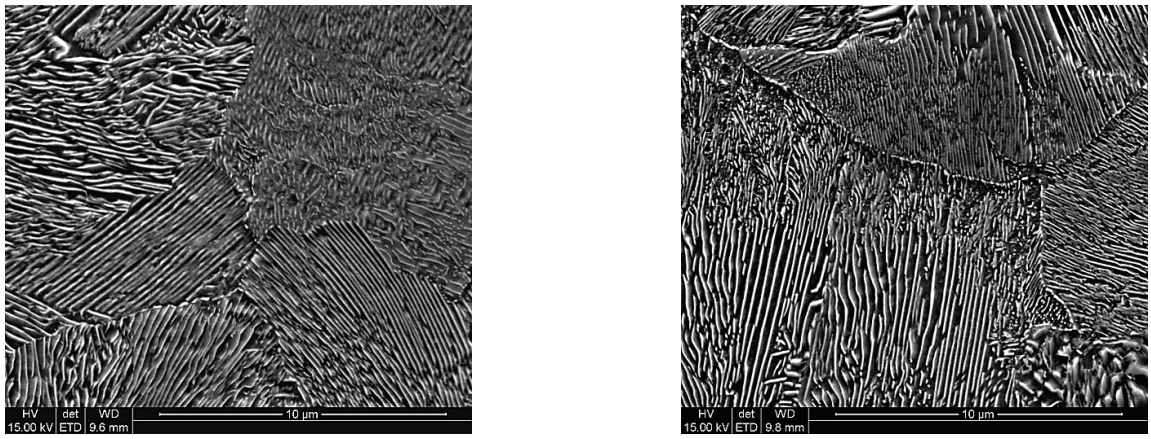

a) *b)*

Fig. 11. *Microstructures for the rail UIC60 for the tests 3 (left) and 4 (right) – scanning microscopy.*

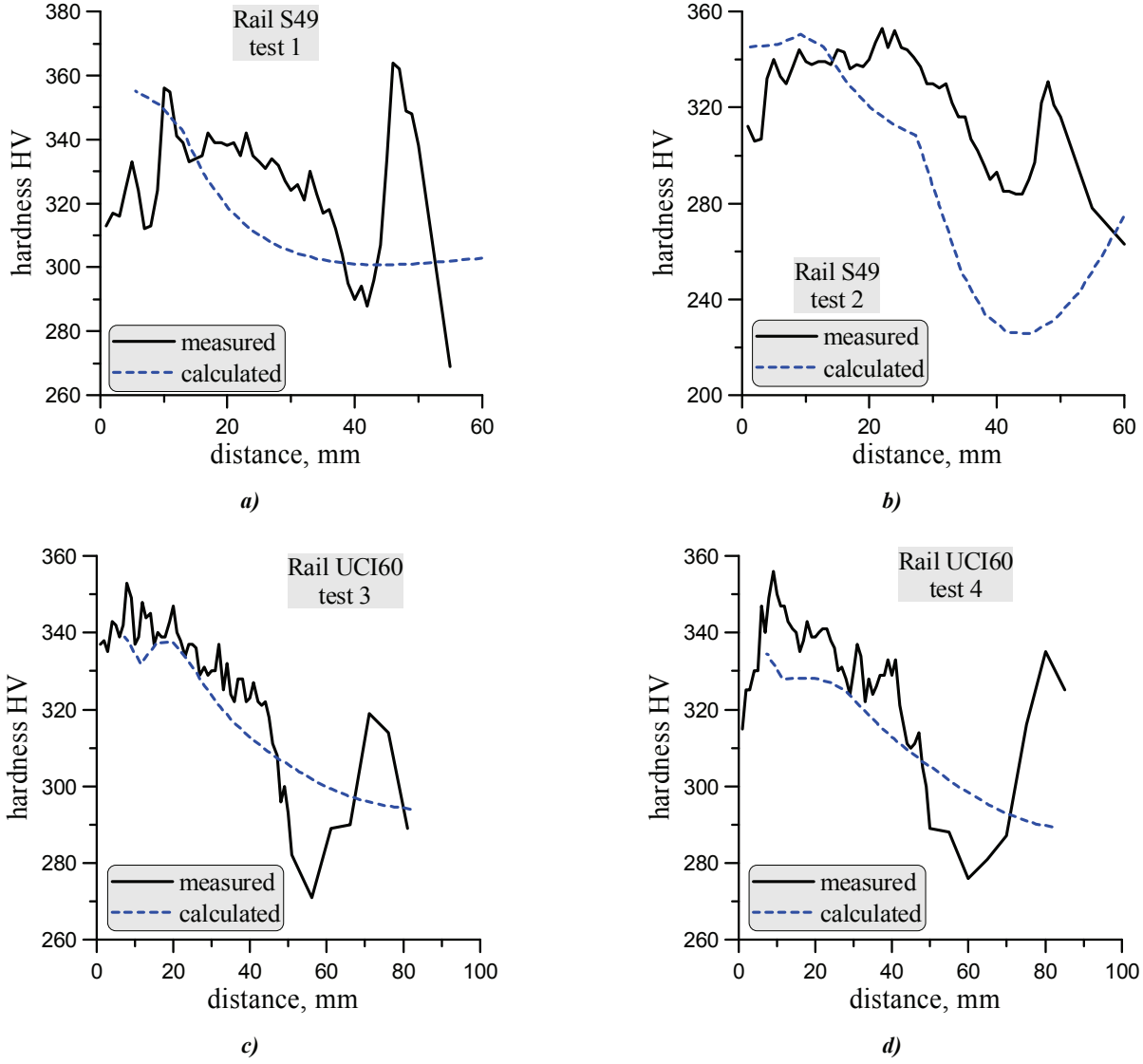

a) *b)* *c)* *d)*

Fig. 12. *Measured and calculated hardness as a function of the distance from the head top surface.*

Measured distributions of the hardness are shown in figure 12. Beyond the small area close to the surface, heterogeneous distribution of the hardness was obtained in the head. A noticeable increase of the hardness was observed in the areas at the connection of the head with the web.

A difference between measured an calculated values of hardness just below the running surface is mainly connected to the decarburization of the head's subsurface layer during heating prior to accelerated cooling. On the contrary, the difference in measured and predicted hardness values in the head's core may be connected to both, too simplified approach to hardness calculation and questionable application of additivity rule for the hardness predictions. These problems are the subject of the current investigation which is being conducted by the authors.

4. CONCLUSIONS

The results of the physical simulations of the controlled cooling of rails were presented in the paper. These results were used for identification, verification and validation of the phase transformation model implemented in the finite element code, which calculated temperatures in rails during cooling. Comparison of measurements and predictions of temperatures, microstructural parameters and mechanical properties confirmed good predictive capabilities of the model. The analysis of results allowed drawing of the following conclusions:

- Water spray cooling gives very intensive drop of the temperature. On the other hand, this method of cooling allows to obtain more uniform heat transfer and more uniform microstructure can be obtained. Thus, this method when better controlled has a potential of improvement of the rail head properties.
- Small difference of the stop temperature of the accelerated cooling results in noticeable difference of microstructural parameters and mechanical properties.
- More complex model for the pearlite microstructure parameters and mechanical properties predictions must be developed to improve the accuracy of the predictions, Specifically, the additivity rule application must be validated for the mechanical properties predictions
- Analysis of the results presented in the paper shows that four parameters of the cooling process should be selected as the independent variables in the optimization: heat transfer coefficient for cooling in the polymer solution, depth of immersion of the rail head, time of fast cooling in the polymer solution and time of cooling in the air at the second stage of cooling.

ACKNOWLEDGEMENTS

Financial assistance of the NCBiR project no. R07 0006 10 is acknowledged.

REFERENCES

Ackert, R.J., Nott, M.A., 1987, Accelerated water cooling of railway rails in-line with the hot rolling mill, *Proc. Symp. Accelerated Cooling of Roled Steels*, eds, Ruddle, G.E., Crawley, A.F., Pergamon Press, Winnipeg, 359-372.

Boyadiev, I.I., Thomson, P.F., Lam, Y.C., 1996, Computation of the diffusional transformation of continuously cooled austenite for predicting the coefficient of thermal expansion in the numerical analysis of thermal stress, *ISIJ International*, 36, 1413-1419.

Garbarz, B., Pickering, F.B., 1988, Effect of pearlite morphology on impact toughness of eutectoid steel containing vanadium, *Materials Science and Technology*, 4, 328-334.

Koistinen, D.P., Marburger, R.E., 1959, A general equation prescribing the extent of the austenite-martensite transformation in pure iron-carbon alloys and plain carbon steels, *Acta Metallurgica*, 7, 59-69.

Kuziak, R., Cheng, Y.-W., Głowacki, M., Pietrzyk, M., 1997, Modelling of the microstructure and mechanical properties of steels during thermomechanical processing, *NIST Technical Note 1393*, Boulder.

Kuziak, R., Zygmunt, T., 2012, A new method of rail head hardening of standard-gauge rails for improved wear and damage resistance, *Steel Research International*, 84, 13-19.

Lenard, J.G., Pietrzyk, M., Cser, L., 1999, *Mathematical and physical simulation of the properties of hot rolled products*, Elsevier, Amsterdam.

Morales, R.D., Lopez, A.G., Olivares, I.M., 1990, Heat transfer analysis during water spray cooling of steel rods, *ISIJ International.*, 30, 48-57.

Perez-Unzueta, A.J., Beynon, J.H., 1993, Microstructure and wear resistance of pearlitic rail steels, *Wear*, 162-164, 173-182,

Pietrzyk, M., Kuziak, R., 2000, Modeling of controlled cooling of rails after hot rolling, *Proc. Conf. Rolling 2000*, Vasteros, CD ROM.

Pietrzyk, M., Kondek, T., Majta, J., Zurek, A.K., Method of identification of the phase transformation model for steels, *Proc. COM 2000*, Ottawa, 2000, CD ROM.

Pietrzyk, M., Kuziak, R., Kondek, T., 2003, Physical and numerical modelling of plastic deformation of steels in two-phase region, *Proc. 45th MWSP Conf.*, Chicago, 209-220.

Pietrzyk, M., Kuziak, R., 2012, Numerical simulation of controlled cooling of rails as a tool for optimal design of this process, *Computer Methods in Materials Science*, 12, 233-243.

Sahay, S.S., Mohapatra, G., Totten, G.E., 2009, Overview of pearlitic rail steels: accelerated cooling, quenching, microstructure and mechanical properties, *Journal of ASTM International*, 6, 1-26.

Scheil, E., 1935, Anlaufzeit der Austenitumwandlung, *Archiv. für Eissenhüttenwesen*, 12, 565-567.

Szeliga, D., Gawąd, J., Pietrzyk, M., 2006, Inverse analysis for identification of rheological and friction models in metal forming, *Computer Methods in Applied Mechanics and Engineering*, 195, 6778-6798.

Umemoto, M., Hiramatsu, A., Moriya, A., Watanabe, T., Nanba, S., Nakajima, N., Anan, G., Higo, Y., 1992, Computer modelling of phase transformation from work-hardened austenite, *ISIJ International*, 32, 306-315.

DOŚWIADCZALNA WERYFIKACJA I WALIDACJA MODELU PRZEMIAN FAZOWYCH STOSOWANEGO DO OPTYMALIZACJI KONTROLOWANEGO CHŁODZENIA SZYN

Streszczenie

Identyfikację modelu przemian fazowych dla stali eutektoidalnej przeprowadzono na podstawie prób dylatometrycznych i analizy odwrotnej. W pracy przeprowadzono fizyczne symulacje kontrolowanego chłodzenia główki szyny po walcowaniu. Wyznaczono parametry mikrostruktury oraz własności mechaniczne po różnych cyklach cieplnych i te dane wykorzystano do weryfikacji i walidacji modelu. W konsekwencji opracowany został wiarygodny model kontrolowanego chłodzenia główki szyny. Ten model może zostać zastosowany do w rozwiązaniu zadania optymalizacyjnego z funkcją celu sformułowaną jak osiągnięcie minimalnych odległości międzypłytkowych w perlicie, zminimalizowanie udziału bainitu w stali i osiągnięcie możliwie równomiernego rozkładu twardości na przekroju szyny.

Received: October 28, 2012
Received in a revised form: November 21, 2012
Accepted: December 2, 2012